

# Topological Recursion for Symplectic Volumes of Moduli Spaces of Curves

JULIA BENNETT, DAVID COCHRAN,  
BRAD SAFNUK, & KAITLIN WOSKOFF

## 1. Introduction

Since Kontsevich’s proof [21] of the Witten conjecture [39], there has been a flurry of activity centered around the tautological ring of the moduli space of curves and expanded more generally to Gromov–Witten invariants. However, many of the fundamental tools developed by Kontsevich have remained comparatively ignored.

In this paper we focus on the combinatorially defined 2-form  $\Omega_{\mathbf{L}}$  used by Kontsevich to represent the scaled sum of  $\psi$ -classes

$$[\Omega_{\mathbf{L}}] = \frac{1}{2}(L_1^2\psi_1 + \cdots + L_n^2\psi_n).$$

In particular, this form leads to a family of symplectic structures on the moduli space of curves, with the associated volumes encoding all possible  $\psi$ -class intersection numbers. Although the nondegeneracy of  $\Omega$  appeared in Kontsevich’s original work, the symplectic nature of  $\Omega$  was not exploited in any particular way.

We develop a recursive formula (an example of *topological recursion*, as explained hereafter) for calculating the symplectic volume of the moduli space of curves. In particular, if  $\text{Vol}_{g,n}(L_1, \dots, L_n)$  represents the symplectic volume of  $\overline{\mathcal{M}}_{g,n}$  calculated with respect to the symplectic form  $\Omega_{\hat{L}}$ , then we have the following statement.

**THEOREM 1.1.** *The symplectic volumes of moduli spaces of curves obey the recursion relation*

$$\begin{aligned} &L_1 \text{Vol}_{g,n}(L_1, \dots, L_n) \\ &= \sum_{j=2}^n \int_{|L_1-L_j|}^{L_1+L_j} dx \frac{x}{2}(L_1 + L_j - x) \text{Vol}_{g,n-1}(x, L_2, \dots, \hat{L}_j, \dots, L_n) \\ &\quad + \sum_{j=2}^n \int_0^{|L_1-L_j|} dx x f(x, L_1, L_j) \text{Vol}_{g,n-1}(x, L_2, \dots, \hat{L}_j, \dots, L_n) \end{aligned}$$

---

Received October 15, 2010. Revision received April 25, 2011.

B.S. would like to thank Motohico Mulase and Yongbin Ruan for helpful comments and suggestions.

Part of the research for this work was conducted as part of Central Michigan University’s REU program in the summer of 2009. J.B., D.C., and K.W. were partially supported by NSF-REU Grant no. DMS 08-51321.

$$\begin{aligned}
 &+ \iint_{0 \leq x+y \leq L_1} dx dy \frac{xy}{2} (L_1 - x - y) \text{Vol}_{g-1, n+1}(x, y, L_2, \dots, L_n) \\
 &+ \sum_{\substack{g_1+g_2=g \\ \mathcal{I} \sqcup \mathcal{J} = \mathbb{n} \setminus 1}} \iint_{0 \leq x+y \leq L_1} dx dy \frac{xy}{2} (L_1 - x - y) \text{Vol}_{g_1, n_1}(x, L_{\mathcal{I}}) \text{Vol}_{g_2, n_2}(y, L_{\mathcal{J}})
 \end{aligned} \tag{1.1}$$

subject to the initial conditions

$$\text{Vol}_{0,3}(L_1, L_2, L_3) = 1, \tag{1.2}$$

$$\text{Vol}_{1,1}(L) = \frac{1}{48} L^2, \tag{1.3}$$

and  $\text{Vol}_{g,n}(L_1, \dots, L_n) = 0$  for  $2g - 2 + n \leq 0$ .

The key technique used in the proof involves constructing Hamiltonian torus actions that act locally on moduli space (see [36] for a related but different toric symmetry on moduli of curves).

We show that the recursion (1.1) has, as a simple corollary, the DVV formula [6] for  $\psi$ -class intersections:

$$\begin{aligned}
 \langle \tau_{d_1} \cdots \tau_{d_n} \rangle_g &= \sum_{j=2}^n \frac{(2d_1 + 2d_j - 1)!!}{(2d_1 + 1)!! (2d_j - 1)!!} \langle \tau_{d_1+d_j-1} \tau_{d_{\mathbb{n} \setminus \{1, j\}}} \rangle_g \\
 &+ \frac{1}{2} \sum_{a+b=d_1-2} \frac{(2a + 1)!! (2b + 1)!!}{(2d_1 + 1)!!} \\
 &\times \left[ \langle \tau_a \tau_b \tau_{d_{\mathbb{n} \setminus 1}} \rangle_{g-1} + \sum_{\substack{\text{stable} \\ g_1+g_2=g \\ \mathcal{I} \sqcup \mathcal{J} = \mathbb{n} \setminus 1}} \langle \tau_a \tau_{d_{\mathcal{I}}} \rangle_{g_1} \langle \tau_b \tau_{d_{\mathcal{J}}} \rangle_{g_2} \right]
 \end{aligned} \tag{1.4}$$

(see Section 5 for notation). This expression yields still another proof of the Witten–Kontsevich theorem.

In addition, defining

$$W_{g,n}(z_1, \dots, z_n) = \int_{\mathbb{R}_+^n} e^{-\sum z_i L_i} \text{Vol}_{g,n}(L_1, \dots, L_n) \prod L_i dL_i$$

and taking the Laplace transform of (1.1) leads us to the equivalent recursion formula

$$\begin{aligned}
 &W_{g,n}(z_1, \dots, z_n) \\
 &= \sum_{j=2}^n -\frac{\partial}{\partial z_j} \left[ \frac{z_j}{(z_1 z_j)^2 (z_1^2 - z_j^2)} (z_1^2 W_{g, n-1}(z_2, \dots, z_n) \right. \\
 &\qquad \qquad \qquad \left. - z_j^2 W_{g, n-1}(z_1, \dots, \hat{z}_j, \dots, z_n) \right] \\
 &+ \frac{1}{2z_1^2} W_{g-1, n+1}(z_1, z_1, \dots, z_n) \\
 &+ \frac{1}{2z_1^2} \sum_{\substack{g_1+g_2=g \\ \mathcal{I} \sqcup \mathcal{J} = \mathbb{n} \setminus 1}} W_{g_1, n_1}(z_1, z_{\mathcal{I}}) W_{g_2, n_2}(z_1, z_{\mathcal{J}}).
 \end{aligned} \tag{1.5}$$

We will prove that (1.5) is an example of the Eynard–Orantin recursion formula [13] for the spectral curve  $x = \frac{1}{2}y^2$ .

We should emphasize that, apart from recursion equation (1.1), none of the results in this paper are new. For example, there are by now many proofs of the Witten–Kontsevich theorem [19; 20; 21; 26; 31; 34; 36], several of which use techniques similar to those employed here. In addition, it has been shown by Eynard and Orantin [15] that the Airy curve encodes the  $\psi$ -class intersection numbers.

Our aim then is not to produce new results in a well-mined field but rather to present a novel point of view with wider applicability and ramifications. For instance, our work makes it geometrically clear *why* it is that the Airy curve encodes intersection numbers—a viewpoint lacking in the literature. In addition, the techniques developed in this paper have a much wider applicability. For example, similar ideas can be used to motivate a generalization of Eynard–Orantin invariants [37] that captures the generalized Kontsevich matrix model (and, in the process, intersection numbers of  $\psi$ -classes over Witten cycles) as well as intersection theory for  $r$ -spin curves. And even though the Airy curve is the simplest nontrivial example of the Eynard–Orantin invariants, it is universal in the sense that (locally) all spectral curves look like the Airy curve. A clear understanding of the local structure of Eynard–Orantin invariants allows one to extrapolate to arbitrary spectral curves by a perturbation-type argument [30]. It should also be pointed out that the recursion formula proven here plays an important role in deriving a new proof [5] of Kontsevich’s integration constant  $\rho = 2^{5g-5+2n}$ , which first appeared in [21] and relates the symplectic volume of the ribbon graph complex to the Euclidean push-forward measure.

This paper is organized as follows. In Section 2 we survey the definitions and constructions needed in the paper. We define the ribbon graph complex and the symplectic 2-form  $\Omega$  originally constructed by Kontsevich. We discuss the relationship to tautological classes on the moduli space of stable curves and also consider the Eynard–Orantin invariants, focusing on the relevant case of when the spectral curve is  $\mathbb{P}^1$ . Finally, we survey the tools from symplectic geometry that will be necessary in the sequel. In particular, we extend the usual symplectic reduction construction to the case of locally defined torus actions with an appropriate partition of unity. In Section 3, we construct the local torus symmetries on the ribbon graph complex and show that the associated symplectic quotients are also ribbon graph complexes. In Section 4, we use the local picture to derive recursion equation (1.1) and provide full consideration of the base-case volumes (1.2) and (1.3). In Section 5 we prove that our recursion relation is equivalent to the DVV equation (Virasoro constraint) for  $\psi$ -class intersections on  $\bar{\mathcal{M}}_{g,n}$ , and in Section 6 we prove that it is equivalent to the Eynard–Orantin recursion for the spectral curve  $x = \frac{1}{2}y^2$ .

## 2. Background

### 2.1. Ribbon Graph Complexes

A ribbon graph is a graph with a cyclic ordering assigned to the half-edges incident on each vertex. The cyclic ordering allows the edges of the graph to be fattened in

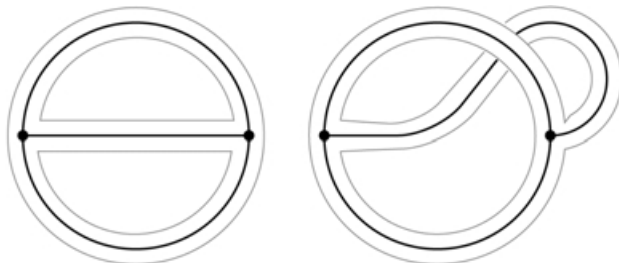


**Figure 1** Ribbons graphs of type  $(0, 3)$  and  $(1, 1)$

a canonical way into ribbons, where the resulting surface has an orientation that induces the cyclic ordering at each vertex. Some examples, along with the associated surfaces, are presented in Figure 1, where the cyclic ordering is implied from the standard counterclockwise orientation of the plane.

A more precise way of defining ribbon graphs that also better elucidates their automorphisms is based on using permutation data. Let  $\gamma \in S_k$  be a permutation of the set  $\underline{k} = \{1, 2, \dots, k\}$ . Then the notation  $(\gamma)$  represents the set of disjoint orbits or cycles of  $\gamma$  and  $|(\gamma)|$  denotes the number of orbits. For example, if  $\gamma = (134)(2)(56)$  then  $(\gamma) = \{(134), (2), (56)\}$  and  $|(\gamma)| = 3$ .

**DEFINITION 2.1.** A ribbon graph is a collection  $(\gamma_0, \gamma_1, \gamma_2, b)$  such that:

- (1) each  $\gamma_i$  is a permutation in  $S_{2k}$  for some fixed  $k > 0$ ;
- (2)  $\gamma_1$  is a fixed point-free involution;
- (3)  $\gamma_0$  contains no cycles of length 1 or 2;
- (4)  $\gamma_2 = \gamma_0^{-1} \circ \gamma_1$  and so, strictly speaking, is not necessary in the definition of the ribbon graph;
- (5)  $b: (\gamma_2) \rightarrow \{1, 2, \dots, |(\gamma_2)|\}$  is a bijection; and
- (6) the group generated by  $\gamma_0$  and  $\gamma_1$  acts transitively on  $\underline{2k}$ .

The map  $b$  is called the *boundary labeling* of the graph, which will become clear in what follows. We also have the numbers  $n = |(\gamma_2)|$ ,  $e = |(\gamma_1)|$ , and  $v = |(\gamma_0)|$ . The *type* of the ribbon graph is the pair  $(g, n)$ , where

$$g = 1 - \frac{1}{2}(v - e + n).$$

To associate this definition with an actual graph, we identify  $(\gamma_0)$  with the set of vertices of our graph,  $(\gamma_1)$  with the set of edges, and  $(\gamma_2)$  with the set of boundary paths. In particular, we take  $|(\gamma_0)|$  vertices and to each vertex we attach a number of half-edges equal to the length of the corresponding cycle in  $\gamma_0$ . Each vertex can be cyclically ordered by  $\gamma_0$ . The half-edges are glued to each other by using  $\gamma_1$ . The construction of a ribbon graph from permutation data is illustrated in Figure 2.

Note that a ribbon graph constructed in this way has its half-edges labeled; however, we do not wish to distinguish ribbon graphs that differ only by their half-edge

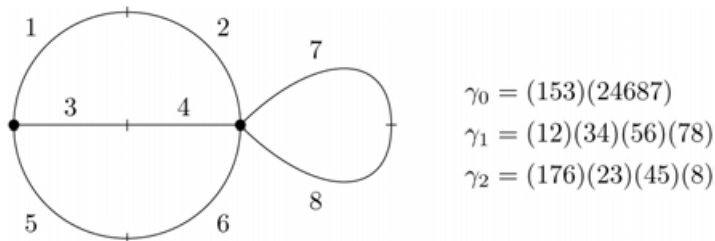


**Figure 2** Constructing a ribbon graph from half-edge permutations

labelings. This preference motivates the notion of equivalence of ribbon graphs: Two ribbon graphs  $(\gamma_0, \gamma_1, b)$  and  $(\gamma'_0, \gamma'_1, b')$  are *equivalent* if there is a bijection  $\alpha: \underline{2k} \rightarrow \underline{2k}$  such that  $\gamma'_i \circ \alpha = \alpha \circ \gamma_i$  and  $b = b' \circ \alpha$ .

One can, in a canonical way, construct an oriented surface from a ribbon graph by first replacing each vertex neighborhood with an oriented disk and then using the edges to attach the disks to each other by ribbons, making sure to preserve the orientation at each vertex. Figure 1 illustrates two ribbon graphs with their associated surfaces. It is straightforward to verify that the surface associated to a given ribbon graph has genus  $g$  and  $n$  holes, which explains the definition of the type of a graph. Note that condition (6) in the definition forces the graph (and hence the surface) to be connected. There are circumstances under which a disconnected ribbon graph is allowed, but the changes to the theory are minor and easily worked out.

In what follows, if  $j \in \underline{2k}$  then the vertex incident to the half-edge  $j$  is denoted  $[j]_0$ . This can also be thought of as the cycle of  $\gamma_0$  that contains  $j$ . Similarly, the edge containing  $j$  is denoted  $[j]_1$  and the corresponding boundary component is  $[j]_2$ . We see that the valence or degree of a vertex (i.e., the number of half-edges incident to it) equals the size of its  $\gamma_0$  orbit. In particular, condition (3) requires that a ribbon graph have no 1- or 2-valent vertices.

We define  $\mathcal{G}_{g,n}$  to be the set of all equivalence classes of ribbon graphs of type  $(g, n)$ . Because of the degree restriction on vertices that results from condition (3), there is an upper bound of  $12g - 12 + 6n$  on the number of half-edges of a graph; this bound is realized exactly when the graph is *trivalent*—in other words, when all vertices have degree 3. As a result, there are a finite number of equivalence classes of graphs of a fixed type. Note that, in general, a ribbon graph  $G \in \mathcal{G}_{g,n}$  may have automorphisms (self-equivalences), and we let  $\text{Aut}(G)$  denote the automorphism group of  $G$ . For example:  $\mathcal{G}_{1,1}$  consists of two graphs, as pictured in Figure 3, with automorphism groups  $\text{Aut}(G_1) = \mathbb{Z}_6$  and  $\text{Aut}(G_2) = \mathbb{Z}_4$ ; and  $\mathcal{G}_{0,3}$  consists of seven distinct graphs, presented in Figure 4, all with trivial automorphism groups. Note that the graphs have nontrivial automorphisms that permute the boundaries, which reduces the number of distinct boundary labelings.

A metric on a ribbon graph  $G = (\gamma_0, \gamma_1, b)$  is a function  $\ell: (\gamma_1) \rightarrow \mathbb{R}_+$  from the set of edges to the positive reals. One can think of a metric as determining the length of each edge of a graph. Observe that if  $e = |(\gamma_1)|$  is the number of edges of  $G$ , then an element of  $\mathbb{R}_+^e$  determines a metric on  $G$ . If  $G$  has nontrivial

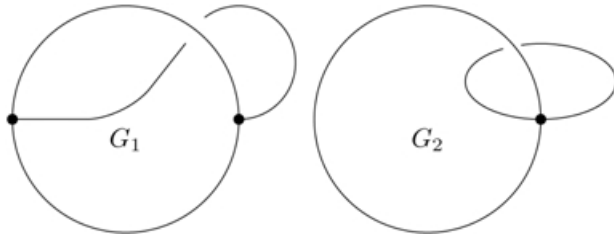


**Figure 3** Set of all ribbon graphs of type (1, 1)

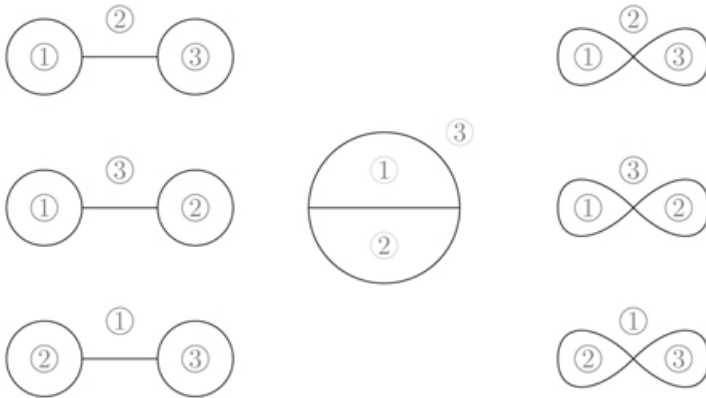


**Figure 4** Set of all ribbon graphs of type (0, 3); boundary labels are indicated by the circled numbers

automorphisms, they act nontrivially on  $\mathbb{R}_+^e$  by permuting the coordinates. Hence we see that the set of all metrics on a graph is naturally identified with

$$\text{Met}(G) = \mathbb{R}_+^e / \text{Aut}(G),$$

and we define the ribbon graph complex of type  $(g, n)$  by

$$\text{RG}_{g,n} = \bigsqcup_{G \in \mathcal{G}_{g,n}} \text{Met}(G).$$

The ribbon graph complex can be given a topology by considering edge collapsing: taking the limit of an edge length to 0, for any nonloop edge, results in a ribbon graph of the same type with the corresponding edge contracted. The resulting set of metric ribbon graphs is glued to the face of the metric set of the larger graph. The resulting topological space has the structure of a connected differentiable orbifold of dimension  $6g - 6 + 3n$  [27; 38].

Given a metric ribbon graph, one can assign perimeters to each boundary of the graph by adding together the lengths of all edges that appear on the boundary. In general, each edge appears on two boundaries (each half-edge is part of a boundary), so it is possible for an edge to contribute twice to a perimeter. We denote the perimeter map

$$p: \text{RG}_{g,n} \rightarrow \mathbb{R}_+^n.$$

Let  $L_{\underline{n}} = (L_1, \dots, L_n) \in \mathbb{R}_+^n$ ; then we define

$$\text{RG}_{g,n}(L_{\underline{n}}) = p^{-1}(L_{\underline{n}}).$$

In other words, it is the set of metric ribbon graphs with fixed boundary lengths.

For  $\Gamma \in \text{RG}_{g,n}$  a metric ribbon graph with half-edge  $i \in \underline{2k}$ , we denote the length of the edge  $[i]_1$  by  $\ell(\Gamma, i)$ ; if the graph is clear from the context then we will use  $\ell_i = \ell(\Gamma, i)$ . In addition, the ribbon graph underlying  $\Gamma$  will be denoted by  $|\Gamma|$ . We can think of the  $\ell_i$  as a set of functions (or local coordinates if we choose one  $i$  for each edge) defined on  $\text{Met}(\Gamma)$ .

Let  $d(i)$  denote the degree of the vertex  $[i]_0$ . To each half-edge  $i$  we associate the vector field

$$\tau_i = \sum_{j=1}^{d(i)-1} (-1)^j \frac{\partial}{\partial \ell_{\gamma_0^j i}}.$$

We also define vector fields assigned to each edge:

$$T_i = T_{\gamma_1 i} = \tau_i + \tau_{\gamma_1 i}.$$

In addition to the orbit notation  $[i]_j$  described previously for vertices, edges, and boundaries of a ribbon graph, we also introduce the following edge-length notation: If boundary  $k$  contains  $m_k$  half-edges, we label the lengths of those edges by  $\ell_1^{[k]}, \dots, \ell_{m_k}^{[k]}$ . The total ordering of the edges must preserve the inherent cyclic ordering of the boundary, but a choice has been made in creating this list (i.e., choosing a distinguished starting edge from the cyclically ordered boundary edges).

Following Kontsevich [21], we construct  $n$  2-forms on the ribbon graph complex (one for each boundary) by

$$\omega_k = \sum_{i=1}^{m_k-1} \sum_{j=i+1}^{m_k} d\ell_i^{[k]} \wedge d\ell_j^{[k]}$$

and then set

$$\Omega = \frac{1}{2} \sum_{k=1}^n \omega_k.$$

Note that  $\Omega$  is not invariant under changes in the choices of total ordering at each boundary. However, the difference is always an exact form with

$$\Omega - \Omega' = \sum_{i=1}^n a_i dp_i,$$

where the  $a_i$  are constants. Hence  $\Omega|_{\text{RG}_{g,n}(L_{\underline{n}})}$  is well-defined, and Kontsevich [21] proved that it is nondegenerate when restricted to cells corresponding to graphs with no even-valent vertices.

We are thus led to define

$$\text{Vol}_{g,n}(L_n) = \int_{\text{RG}_{g,n}(L_n)} e^\Omega = \int_{\text{RG}_{g,n}(L_n)} \frac{1}{d!} \Omega^d,$$

where  $d = 3g - 3 + n$ .

In general, the dimension of  $\text{RG}_{g,n}$  is equal to  $6g - 6 + 3n$ , which corresponds to the number of edges in a trivalent ribbon graph (all vertices have degree 3). Because they play a special role in what follows, we use  $\text{RG}_{g,n}^3$  to denote the space of trivalent metric ribbon graphs. Although  $\Omega^d$  is not, strictly speaking, a volume form—since it is degenerate on ribbon graphs with even-valent vertices—it is non-degenerate on the top-dimension strata  $\text{RG}_{g,n}^3(L_n)$ . Because integration over a set of measure 0 does not contribute, the volume is well-defined.

### 2.2. Intersection Theory on $\overline{\mathcal{M}}_{g,n}$

The primary motivation for studying the ribbon graph complex is its close connection to the moduli space of curves  $\mathcal{M}_{g,n}$ , which is the set of all smooth algebraic curves of genus  $g$  that have  $n$  distinguished, labeled points. In fact, a result variously attributed to Mumford, Thurston, or Harer [18] states that  $\mathcal{M}_{g,n} \times \mathbb{R}_+^n$  is diffeomorphic (in the sense of orbifolds) to  $\text{RG}_{g,n}$ . This result follows by examining foliations from Strebel differentials on surfaces. A similar result was proved by Bowditch and Epstein [4] and independently by Penner [35], who used hyperbolic geometry.

These results were utilized by Kontsevich [21] to great effect in his celebrated proof of the Witten conjecture [39]. By careful analysis of degenerating ribbon graphs, he was able to use the ribbon graph complex in calculating intersection numbers over the Deligne–Mumford compactification of moduli space  $\overline{\mathcal{M}}_{g,n}$ . To be precise, there is a compactification of the ribbon graph complex  $\overline{\text{RG}}_{g,n}(L)$  on which the symplectic form  $\Omega$  extends as well as a map

$$q: \overline{\mathcal{M}}_{g,n} \rightarrow \overline{\text{RG}}_{g,n}(L)$$

for which  $q^*\Omega$  represents the sum tautological classes  $\frac{1}{2}(L_1^2\psi_1 + \dots + L_n^2\psi_n)$ . The cohomology class  $\psi_i \in H^2(\overline{\mathcal{M}}_{g,n}; \mathbb{Q})$  is defined to be the first Chern class of the line bundle  $\mathcal{L}_i$ , which (roughly speaking) is the line bundle whose fiber over the point  $(C, p_1, \dots, p_n) \in \overline{\mathcal{M}}_{g,n}$  is  $T_{p_i}^*C$  for  $C$  a stable algebraic curve with marked points  $p_1, \dots, p_n$ .

Hence, one interpretation of the symplectic volume discussed in the previous section is that it encodes all intersections of  $\psi$ -classes on  $\overline{\mathcal{M}}_{g,n}$ . In fact,

$$\text{Vol}_{g,n}(L_N) = \sum_{k_1 + \dots + k_n = d} \prod_{j=1}^n \frac{L_j^{2k_j}}{2^{k_j} k_j!} \int_{\overline{\mathcal{M}}_{g,n}} \psi_1^{k_1} \dots \psi_n^{k_n}. \tag{2.1}$$

### 2.3. Eynard–Orantin Topological Recursion

The topological recursion formula presented in Section 4 fits into the framework developed by Eynard and Orantin [13], which we now proceed to outline.

Consider a plane algebraic curve  $C$  specified by a polynomial equation

$$C^o = \{(x, y) \in \mathbb{C}^2 \mid P(x, y) = 0\},$$

$$C = \overline{C^o}.$$

It is convenient to think of  $x$  and  $y$  as a choice of two meromorphic functions on  $C$ . In other words, given a local coordinate  $z \in C$  we have

$$x = x(z),$$

$$y = y(z).$$

We require that the projection of  $C$  onto the  $x$ -axis be *generic*: branch points must be isolated and of degree at most 2 (simply ramified).

We remark that the theory developed by Eynard and Orantin applies in a wider setting than presented here, but restricting  $x$  and  $y$  to be rational functions is more than sufficient for our needs and makes the theory somewhat simpler. In what follows, we make the additional (unnecessary) assumption that  $C = \mathbb{P}^1$  with global coordinate  $z$ .

To the data of a spectral curve we can associate an infinite tower of symmetric multilinear meromorphic differentials  $\mathcal{W}_{g,n}(z_1, \dots, z_n) = W_{g,n}(z_1, \dots, z_n) dz_1 \otimes \dots \otimes dz_n$  defined on  $\text{Sym}^n C$ . They are constructed by recursively performing residue computations around the branch points of the  $x$ -projection.

In particular, the base cases of the recursion are

$$\mathcal{W}_{0,1}(z) = 0,$$

$$\mathcal{W}_{0,2}(z_1, z_2) = \frac{dz_1 \otimes dz_2}{(z_1 - z_2)^2};$$

here  $\mathcal{W}_{0,2}$  is the *Cauchy differentiation kernel* defined by the property that, for any meromorphic function  $f : C \rightarrow \mathbb{P}^1$ ,

$$f'(z) dz = \text{Res}_{\zeta \rightarrow z} f(\zeta) \mathcal{W}_{0,2}(\zeta, z).$$

This differentiation kernel is also referred to as the *Bergmann kernel* in the literature [13]. In addition, if  $C$  has genus greater than 0, then the  $\mathcal{A}$ -cycle integrals of the kernel must be specified in order to have a unique bilinear differential.

A few additional constructions are necessary to derive the higher-order invariants. The first is a notion of *conjugate point*. Let  $a_1, \dots, a_k$  be the branch points of the projection of  $C$  onto the  $x$ -axis. If  $z \in C$  is sufficiently close to a branch point  $a_i$ , then there is a unique point  $\bar{z} \neq z$  with the same  $x$ -projection as  $z$  (because all branch points are simple). Observe that, unlike complex conjugation, the locally defined involution  $z \mapsto \bar{z}$  is holomorphic.

We also make use of the *Eynard kernel*, defined as

$$E_i(z_1, z_2) = \frac{1}{2} \int_{z_1}^{\bar{z}_1} \mathcal{W}_{0,2}(\zeta, z_2) d\zeta \frac{dz_2}{(y(z_1) - y(\bar{z}_1)) dx(z_1)},$$

where  $E_i$  is defined locally around the branch point  $a_i$  (from which the conjugation operation is defined) and the operator on differential forms  $\frac{1}{dx(z)}$  is equivalent to contraction on the vector field

$$\frac{1}{dx/dz} \frac{d}{dz}.$$

Then the higher-order Eynard–Orantin invariants are defined by the recursion formula

$$\begin{aligned} \mathcal{W}_{g,n+1}(z, z_n) &= \sum_i \operatorname{Res}_{\zeta \rightarrow a_i} E_i(z, \zeta) \left[ \mathcal{W}_{g-1, n+2}(\zeta, \bar{\zeta}, z_n) \right. \\ &\quad \left. + \sum_{g_1+g_2=g} \sum_{\mathcal{I} \sqcup \mathcal{J} = n} \mathcal{W}_{g_1, |\mathcal{I}|+1}(\zeta, z_{\mathcal{I}}) \mathcal{W}_{g_2, |\mathcal{J}|+1}(\bar{\zeta}, z_{\mathcal{J}}) \right]. \end{aligned}$$

The Eynard–Orantin invariants have appeared in a broad array of seemingly unconnected mathematics. Some highlights are listed next.

- (1) The correlation functions for  $y = \sin(\sqrt{x})$  are related (via the Laplace transform) to the Weil–Petersson symplectic volumes for moduli spaces of bordered Riemann surfaces [14], and the recursion formula is equivalent to the recursion formula first discovered by Mirzakhani [25; 26] in the context of hyperbolic geometry.
- (2) The recursion for intersection numbers of mixed  $\psi$  and  $\kappa_1$  classes originally discovered by Mulase and Safnuk [29] and then extended to arbitrary  $\kappa$  classes by Liu and Xu [22; 23; 24] were put into the framework of topological recursion by Eynard [8].
- (3) Topological recursion can be used to calculate the generating function that enumerates partitions with the Plancherel measure [9; 10].
- (4) Correlation functions for the curve of the mirror dual to a 3-dimensional toric Calabi–Yau manifold are conjectured to generate the Gromov–Witten potential of the manifold. [2; 11; 16].
- (5) The Lambert curve  $x = ye^{-x}$  yields the generating functions for Hurwitz numbers [1; 3; 12], giving a positive resolution to a conjecture raised by Bouchard and Mariño [3].
- (6) The curve  $x = y + 1/y$  was shown by Norbury [32; 33] to compute the number of lattice points in the moduli space of curves; see [5; 28] for a related construction.

The simplest nontrivial example of a spectral curve is the Airy curve

$$\begin{aligned} x &= \frac{1}{2}z^2, \\ y &= z, \end{aligned}$$

which is a rational curve with global coordinate  $z$ . There is a single branch point at  $(0, 0)$  with a globally defined involution  $z \mapsto -z$ .

The Cauchy differentiation kernel for the Riemann sphere is given by

$$\mathcal{W}_{0,2}(z_1, z_2) = \frac{dz_1 \otimes dz_2}{(z_1 - z_2)^2},$$

and the Eynard kernel at the unique branch point is

$$E(z_1, z_2) = \frac{1}{z_1^2 - z_2^2} \frac{dz_2}{2z_1 dz_1}.$$

This yields a recursion formula

$$\begin{aligned} & \mathcal{W}_{g,n}(z_1, \dots, z_n) \\ &= \operatorname{Res}_{\zeta \rightarrow 0} \frac{dz_1}{2\zeta(\zeta^2 - z_1^2) d\zeta} \left( \mathcal{W}_{g-1,n+1}(\zeta, -\zeta, z_2, \dots, z_n) \right. \\ & \quad \left. + \sum_{\substack{g_1+g_2=g \\ \mathcal{I} \sqcup \mathcal{J} = \underline{n} \setminus \{1\}}} \mathcal{W}_{g_1,n_1}(\zeta, z_{\mathcal{I}}) \mathcal{W}_{g_2,n_2}(-\zeta, z_{\mathcal{J}}) \right). \end{aligned} \quad (2.2)$$

Now applying the Eynard–Orantin recursion to the first few cases gives

$$\begin{aligned} \mathcal{W}_{0,3}(z_1, z_2, z_3) &= \frac{dz_1 \otimes dz_2 \otimes dz_3}{z_1^2 z_2^2 z_3^2}, \\ \mathcal{W}_{1,1}(z) &= \frac{dz}{8z^4}, \\ \mathcal{W}_{0,4}(z_1, z_2, z_3, z_4) &= 3 \left( \frac{1}{z_1^2} + \frac{1}{z_2^2} + \frac{1}{z_3^2} + \frac{1}{z_4^2} \right) \prod_{i=1}^4 \frac{dz_i}{z_i^2}. \end{aligned}$$

### 2.4. Symplectic Geometry

The goal of this paper is to calculate the symplectic volume of the ribbon graph complex. The technique presented relies on a slight extension of several standard constructions from symplectic geometry. In particular, we extend the Duistermaat–Heckman measure and symplectic reduction to calculate the volumes when the Hamiltonian torus actions act only locally on the manifold. The local reductions are glued together using an equivariant partition of unity. Details are presented next.

The pair  $(M, \omega)$  is a symplectic manifold if  $M$  is a smooth  $2n$ -manifold and  $\omega$  is a closed, nondegenerate 2-form on  $M$ . The nondegeneracy condition on  $\omega$  forces  $M$  to be even-dimensional. In general, if  $(M, \omega)$  is a symplectic manifold, then the top-dimension form  $\frac{1}{n!} \omega^n$  is everywhere nondegenerate and therefore is a volume form. When  $M$  is compact (or  $\omega^n$  is integrable), we define

$$\operatorname{Vol}(M, \omega) = \int_M \frac{1}{n!} \omega^n.$$

Note in particular that the symplectic volume depends on the form  $\omega$ ; however, when  $M$  is compact the volume is an invariant of the cohomology class of  $\omega$ .

Suppose that  $(M, \omega)$  has a  $k$ -torus symmetry. In particular, suppose there is a  $k$ -parameter group of diffeomorphisms

$$F_{(t_1, \dots, t_k)} : M \rightarrow M$$

that satisfies the following conditions:

- (1)  $F_{(t_1, \dots, t_k)}$  is a symplectomorphism for all  $t = (t_1, \dots, t_k) \in \mathbb{R}^k$  (i.e.,  $F_t^* \omega = \omega$ );
- (2)  $F_t \circ F_{t'} = F_{t+t'}$  for all  $t, t' \in \mathbb{R}^k$ ; and

(3) there exists a  $c \in \mathbb{R}_+^k$  with  $F_{t+c} = F_t$  for all  $t \in \mathbb{R}^k$  (the constant  $c_j$  is the *period* or circumference of the  $j$ th component of the torus action).

Then the symplectic torus action encoded by  $F$  has  $k$  commuting vector fields, denoted  $X_1, \dots, X_k$  and constructed by taking derivatives of  $F$ :

$$X_j(x) = \left. \frac{\partial F_t(x)}{\partial t_j} \right|_{t=0}.$$

A symplectic torus action is called *Hamiltonian* if there is, in addition to the foregoing conditions, a map  $\mu: M \rightarrow \mathbb{R}^k$  (called the moment map) satisfying the duality condition

$$\iota_{X_j} \omega = d\mu_j.$$

Note that  $\iota_X$  is the contraction operator, which takes the  $q$ -form  $\alpha$  to the  $(q - 1)$ -form such that, for any collection of vector fields  $Y_1, \dots, Y_{q-1}$ ,

$$\iota_X \alpha(Y_1, \dots, Y_{q-1}) = \alpha(X, Y_1, \dots, Y_{q-1}).$$

A key property of the moment map is that the torus action preserves level sets:  $F_t \mu^{-1}(a) \subset \mu^{-1}(a)$  for all  $a, t \in \mathbb{R}^k$ . In addition, in many situations the quotient of a level set by the torus is still a manifold. We denote the quotient space

$$M_a = \mu^{-1}(a) / \mathbb{T}^k.$$

In fact, it will be a symplectic manifold with a canonical symplectic form  $\omega_a$  induced from the original symplectic structure. To be precise, let  $q: \mu^{-1}(a) \rightarrow M_a$  be the quotient map. If  $Y_1, Y_2$  are two tangent vectors on  $M_a$ , then we choose arbitrary lifts  $\tilde{Y}_i$  (i.e.,  $q_* \tilde{Y}_i = Y_i$ ) and define

$$\omega_a(Y_1, Y_2) = \omega(\tilde{Y}_1, \tilde{Y}_2).$$

One can check that  $\omega_a$  is well-defined, closed, and nondegenerate.

The construction just described is called *symplectic reduction*. The relevance in the present situation is its applications in volume calculations. Let  $D \subset \mathbb{R}^k$  be the image of the moment map. By a theorem of Guillemin and Sternberg [17],  $D$  is a convex polytope. One can define the Duistermaat–Heckman measure on  $D$  by considering the volume form

$$\text{Vol}(M_x) dx_1 \cdots dx_k.$$

In fact, we have [7]

$$\text{Vol}(M) = \int_D \prod c_i \text{Vol}(M_x) dx_1 \cdots dx_k. \tag{2.3}$$

In the present context, however, the ribbon graph complex does not admit a global circle action. To circumvent this difficulty, we construct a locally finite cover  $\{U_i\}$  and corresponding partition of unity  $\{\phi_i\}$ . We assume that each symplectic manifold  $(U_i, \omega)$  has a Hamiltonian circle action with moment map  $\mu_i: U_i \rightarrow \mathbb{R}$ . (We remark that this discussion can be trivially extended to torus actions, but for ease of notation we suppress such generalities.) The key assumption we are making is that  $\phi_i$  is *equivariant with respect to the circle action on  $U_i$* . Equivalently,

we assume that  $\phi_i$  is constant on the level sets  $\mu_i^{-1}(x)$ . Hence there is a function  $f_i : \mathbb{R} \rightarrow \mathbb{R}$  with  $f_i \circ \mu_i = \phi_i$ .

The goal is to calculate the symplectic volume

$$\int_M \frac{1}{n!} \omega^n,$$

which we first write as a sum of integrals using the partition of unity:

$$\int_M \frac{1}{n!} \omega^n = \sum_i \int_{U_i} \frac{\phi_i}{n!} \omega^n.$$

In order to calculate the integral over  $U_i$ , we utilize the Hamiltonian circle action. Let  $V_i(x) = \mu_i^{-1}(x)/S^1$  be the symplectic quotient with induced symplectic form  $\omega_i(x)$ . Observe that, at this stage, the partition function  $\phi_i$  is not part of the construction. We let  $\text{Vol}_i(x)$  denote the volume of the quotient.

Recall the Duistermaat–Heckman measure on  $\mathbb{R}$ : If  $A \subset \mathbb{R}$  is any measurable subset, we define

$$m_i^{\text{DH}}(A) = \int_{\mu_i^{-1}(A)} \frac{\omega^n}{n!}.$$

In particular, we can integrate the function  $f_i$  with respect to this measure and obtain

$$\int_{\mathbb{R}} f_i(x) m_i^{\text{DH}}(x) = \int_{U_i} \frac{\mu_i^*(f_i)}{n!} \omega^n = \int_{U_i} \frac{\phi_i}{n!} \omega^n.$$

To complete the calculation, we relate the Duistermaat–Heckman measure to ordinary Lebesgue measure with the Radon–Nikodym derivative. According to Duistermaat and Heckman, this derivative is equal to  $\text{Vol}_i(x)$  times the circumference of the circle action. Hence

$$\int_{U_i} \frac{\phi_i}{n!} \omega^n = \int_{\mu_i(U_i)} f_i(x) \theta_i(x) \text{Vol}_i(x) dx,$$

where  $\theta_i(x)$  is the circumference of the circle action at level  $x$ . In this paper that circumference is equal to  $x$ , so the choice of coordinates is analogous to polar coordinates (Cartesian coordinates would have constant circumference).

### 3. Local Structure

In this section we construct locally defined Hamiltonian torus actions on the ribbon graph complex. A careful analysis of the domain on which the group action is defined allows for a partition of unity subordinate to the open cover induced by the various domains. As a consequence, one can derive a formula for the volume of the ribbon graph complex by using the symplectic reduction techniques outlined in Section 2.4. The symplectic quotients are themselves ribbon graph complexes that involve graph types of less complexity (where the *complexity* of a graph of type  $(g, n)$  is equal to  $2g - 2 + n$ ). The result is a recursive formula for calculating the symplectic volumes.

Let  $\Gamma$  be a trivalent metric ribbon graph. Given an edge  $[i]_1$ , we define the metric ribbon graph  $\Gamma_{\hat{i}}$  obtained by removing the edge  $[i]_1$  from  $\Gamma$  and straightening the resultant 2-valent vertices into contiguous edges, as depicted in Figure 5. The edge lengths of  $\Gamma_{\hat{i}}$  are inherited from  $\Gamma$ . There is an exception to this operation when  $[i]_1$  adjoins (or is itself) a loop; in that case,  $\Gamma_{\hat{i}}$  is defined by removing the entire lollipop from  $\Gamma$  (see Figure 6).

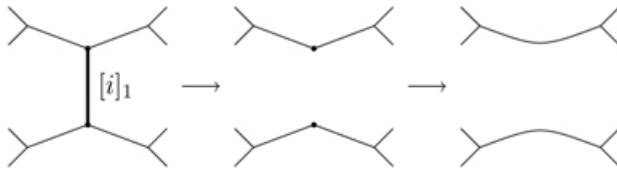


**Figure 5** Edge removal from a trivalent ribbon graph

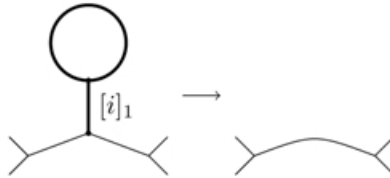


**Figure 6** Removing a lollipop

If we remember the locations of the deleted vertices, we will have two marked points on the boundary of  $\Gamma_{\hat{i}}$ . Let  $m(\Gamma, i)$  denote the number of distinct boundary components on which the markings appear (either 1 or 2). Rotating the marked points can be realized as an  $m$ -torus orbit in  $\text{RG}_{g,n}$  (if  $m = 1$  then the rotations must be synchronized). We consider the lollipop removal case also to have a single marked boundary ( $m = 1$ ), since rotation on a simple loop is a trivial action. We call these rotations edge-twist deformations, as one imagines twisting the edge  $[i]_1$  around its connections to the remainder of the graph. The infinitesimal generators of these deformations are  $T_i$  in the case of a circle action and the pair  $(\tau_i, \tau_{\gamma_i i})$  in the case of a torus action. When edge  $[i]_1$  forms a loop, the relevant vector field is  $T_{\gamma_0 i} + T_{\gamma_0^2 i}$  (exactly one of these two terms is nonzero).

The set of all ribbon graphs obtained during one complete rotation of edge  $[i]_1$  is called the *torus orbit* of  $(\Gamma, i)$  and is denoted  $\mathcal{O}(\Gamma, i)$ . For any  $\Gamma \in \text{RG}_{g,n}^3(L_n)$  we consider the set

$$\mathcal{U}(\Gamma, i) = \bigcup_{\tilde{\Gamma} \in \text{Met}(|\Gamma|; L_n)} \mathcal{O}(\tilde{\Gamma}, i),$$

where  $\text{Met}(|\Gamma|; L_n) = \text{RG}_{g,n}(L_n) \cap \text{Met}(|\Gamma|)$ . Note that  $\mathcal{U}(\Gamma, i) \subset \text{RG}_{g,n}(L_n)$ .

Restricting our attention to edges that are adjacent to the first boundary (boundary label 1), we still obtain a cover of the trivalent strata:

$$\text{RG}_{g,n}^3(L_n) \subset \bigcup_{\Gamma \in \text{RG}_{g,n}^3(L_n)} \bigcup_{i: b(i)=1} \mathcal{U}(\Gamma, i).$$

In addition, each subset  $\mathcal{U}(\Gamma, i)$  has a well-defined function  $f_{\Gamma,i}(\tilde{\Gamma}) = \ell(\tilde{\Gamma}, i)$  (i.e., we measure the length of the singled-out edge  $i$ ).

LEMMA 3.1. *The collection of functions  $\{\frac{1}{L_1} f_{\Gamma,i}\}$  forms a partition of unity subordinate to the cover  $\{\mathcal{U}(\Gamma, i) \mid \Gamma \in \text{RG}_{g,n}^3(L_n), b_\Gamma(i) = 1\}$ .*

*Proof.* This follows from observing that the sum of edge lengths around the first boundary equals  $L_1$  by definition. □

We note that, by construction, each  $\mathcal{U}(\Gamma, i)$  has a globally defined torus action. The dimension of the torus is either 1 or 2, depending on the configuration of the vertices incident to edge  $[i]_1$  (as discussed previously).

LEMMA 3.2. *The torus action on  $\mathcal{U}(\Gamma, i)$  is Hamiltonian with moment map given by the period(s) of the action.*

*Proof.* We must calculate the contraction of  $\Omega$  by the vector fields  $\tau_i$  and  $\tau_{\gamma_1 i}$  in the torus action case and by the vector field  $T_i$  in the circle action case. Beginning with the case of the circle action, refer to Figure 7 for the notation used in what follows.

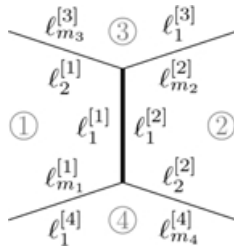


Figure 7 Edge labels used to calculate vector field contraction; the dark vertical edge is  $[i]_1$

The only terms in  $\Omega$  that contribute are  $\omega_i$  for  $i = 1, 2, 3, 4$ . Without loss of generality, we may assume that edge  $[i]_1$  corresponds with  $l_1^{[1]}$  and  $l_1^{[2]}$ , that edge  $[\gamma_0 \gamma_1 i]_1$  corresponds with  $l_1^{[3]}$ , and that edge  $[\gamma_0 i]_1$  corresponds with  $l_1^{[4]}$ . Under this labeling, we have

$$\begin{aligned} T_i &= -\frac{\partial}{\partial \ell_{m_2}^{[2]}} + \frac{\partial}{\partial \ell_2^{[1]}} - \frac{\partial}{\partial \ell_{m_1}^{[1]}} + \frac{\partial}{\partial \ell_2^{[2]}} \\ &= -\frac{\partial}{\partial \ell_1^{[3]}} + \frac{\partial}{\partial \ell_{m_3}^{[3]}} - \frac{\partial}{\partial \ell_1^{[4]}} + \frac{\partial}{\partial \ell_{m_4}^{[4]}}. \end{aligned}$$

It is now straightforward to calculate

$$\begin{aligned}
\iota_{T_i}\omega_1 &= -d\ell_1^{[1]} + (d\ell_3^{[1]} + \cdots + d\ell_{m_1}^{[1]}) + (d\ell_1^{[1]} + \cdots + d\ell_{m_1-1}^{[1]}) \\
&= 2dp_1 - 2d\ell_1^{[1]} - d\ell_2^{[1]} - d\ell_{m_1}^{[1]}, \\
\iota_{T_i}\omega_2 &= 2dp_2 - 2d\ell_1^{[2]} - d\ell_2^{[2]} - d\ell_{m_2}^{[2]}, \\
\iota_{T_i}\omega_3 &= -(d\ell_2^{[3]} + \cdots + d\ell_{m_3}^{[3]}) + (-d\ell_1^{[3]} - \cdots - d\ell_{m_3-1}^{[3]}) \\
&= -2dp_3 + d\ell_1^{[3]} + d\ell_{m_3}^{[3]}, \\
\iota_{T_i}\omega_4 &= -2dp_4 + d\ell_1^{[4]} + d\ell_{m_4}^{[4]}.
\end{aligned}$$

Although it becomes slightly more complicated, nothing changes fundamentally in this calculation if some of the boundaries happen to agree.

Since  $\ell_2^{[1]} = \ell_{m_3}^{[3]}$ ,  $\ell_{m_1}^{[1]} = \ell_1^{[4]}$ ,  $\ell_2^{[2]} = \ell_{m_4}^{[4]}$ ,  $\ell_{m_2}^{[2]} = \ell_1^{[3]}$ , and  $\ell_1^{[1]} = \ell_i = \ell_1^{[2]}$  (being different labels for the same edges), it follows that

$$\iota_{T_i}\Omega = d(p_1 + p_2 - 2\ell_i) - dp_3 - dp_4.$$

When this expression is restricted to  $\text{RG}_{g,n}(L_n)$  we have  $dp_k = 0$ , and the first part of the proof is complete once we observe that  $p_1 + p_2 - 2\ell_i$  is the length of the circle around which edge  $i$  rotates.

The torus action case occurs when edge  $i$  has the same boundary on either side. Refer to Figure 8 for the notation used in what follows.

When traversing boundary 1, we assume that  $\ell_i = \ell_1^{[1]}$  and observe that edge  $i$  divides the perimeter into two distinct regions (which become the two distinct circles for the torus action). We label  $\ell_k^{[1]}$  as the second occurrence of  $\ell_i$  in the perimeter, which yields the two regions labeled by  $\ell_2^{[1]}, \dots, \ell_{k-1}^{[1]}$  and  $\ell_{k+1}^{[1]}, \dots, \ell_{m_1}^{[1]}$ .

The vector fields under this labeling are given by

$$\begin{aligned}
\tau_i &= \frac{\partial}{\partial \ell_2^{[1]}} - \frac{\partial}{\partial \ell_{k-1}^{[1]}} \\
&= \frac{\partial}{\partial \ell_{m_3}^{[3]}} - \frac{\partial}{\partial \ell_1^{[3]}}, \\
\tau_{\gamma_i} &= \frac{\partial}{\partial \ell_{k+1}^{[1]}} - \frac{\partial}{\partial \ell_{m_1}^{[1]}} \\
&= \frac{\partial}{\partial \ell_{m_2}^{[2]}} - \frac{\partial}{\partial \ell_1^{[2]}},
\end{aligned}$$

from which we calculate

$$\begin{aligned}
\iota_{\tau_i}\omega_1 &= -d\ell_1^{[1]} + d\ell_3^{[1]} + \cdots + d\ell_{m_1}^{[1]} + d\ell_1^{[1]} + \cdots + d\ell_{k-2}^{[1]} \\
&\quad - (d\ell_k^{[1]} + \cdots + d\ell_{m_1}^{[1]}) \\
&= 2(d\ell_2^{[1]} + \cdots + d\ell_{k-1}^{[1]}) - d\ell_2^{[1]} - d\ell_{k-1}^{[1]}, \\
\iota_{\tau_i}\omega_3 &= -(d\ell_2^{[3]} + \cdots + d\ell_{m_3}^{[3]}) - (d\ell_1^{[3]} + \cdots + d\ell_{m_3-1}^{[3]}) \\
&= -2dp_3 + d\ell_1^{[3]} + d\ell_{m_3}^{[3]}, \\
\iota_{\tau_{\gamma_i}}\omega_1 &= 2(d\ell_{k+1}^{[1]} + \cdots + d\ell_{m_1}^{[1]}) - d\ell_{k+1}^{[1]} - d\ell_{m_1}^{[1]}, \\
\iota_{\tau_{\gamma_i}}\omega_2 &= -2dp_2 + d\ell_1^{[2]} + d\ell_{m_2}^{[2]}.
\end{aligned}$$

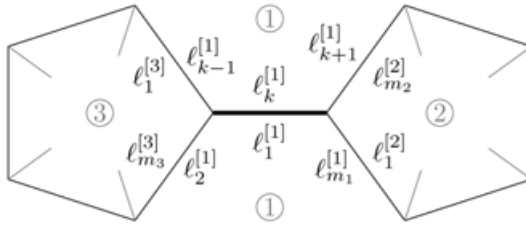


**Figure 8** Edge labels used to calculate vector field contraction; the dark horizontal edge is  $[i]_1$

Canceling same-edge terms then yields

$$\begin{aligned} \iota_{\tau_i} \Omega &= d(\ell_2^{[1]} + \cdots + \ell_{k-1}^{[1]}) - dp_3, \\ \iota_{\tau_{\gamma_i}} \Omega &= d(\ell_{k+1}^{[1]} + \cdots + \ell_{m_1}^{[1]}) - dp_2. \end{aligned}$$

Ignoring the inconsequential  $dp_k$  terms, we observe that  $\ell_2^{[1]} + \cdots + \ell_{k-1}^{[1]}$  is the period of the first circle action and  $\ell_{k+1}^{[1]} + \cdots + \ell_{m_1}^{[1]}$  is the period of the second, thus completing the proof of the lemma.  $\square$

A corollary of this proof is that  $\Omega$  restricted to  $\text{RG}_{g,n}^3(L)$  is nondegenerate. In fact, the vector fields  $T_i$  span the tangent space  $T \text{RG}_{g,n}^3(L)$ , and the duality relation  $\iota_{T_i} \Omega = -2d\ell_i$  completely characterizes  $\Omega$ .

An alternative description of the moment map is the perimeter map for the newly created boundary (or boundaries) obtained by removing edge  $[i]_1$ . Hence the symplectic quotients are identified with subsets of ribbon graph complexes obtained by edge removal. To be precise, the symplectic quotient is a subset of  $\text{RG}_{g',n'}$ , where  $(g', n')$  is the type of the graph  $\Gamma_i$ . If removing  $i$  disconnects  $\Gamma$  into two graphs of type  $(g_1, n_1)$  and  $(g_2, n_2)$ , then the quotient will be a subset of  $\text{RG}_{g_1, n_1} \times \text{RG}_{g_2, n_2}$ . Moreover, the perimeters of the newly created graphs are fixed by the original perimeters of  $\Gamma$  and the particular level of the moment map taken for the quotient. A more precise determination of these perimeters and the types of graphs that appear for the quotient is deferred to Section 4.

One consequence of the geometry of these quotients is that they have two independent symplectic structures:  $\bar{\Omega}$  coming from symplectic reduction, and  $\Omega$  induced from the Kontsevich symplectic form on  $\text{RG}_{g',n'}$ . Although they are defined differently, our next lemma shows that the two symplectic structures agree.

LEMMA 3.3.  $\bar{\Omega} = \Omega$ .

*Proof.* Recall that  $\Omega$  is identified by the duality relation  $\Omega(T_i, \cdot) = -2d\ell_i$  whereas  $\bar{\Omega}$  is calculated by lifting vectors to the torus orbit. We denote the quotient map by  $q: \mathcal{U}(\Gamma, i) \rightarrow \text{RG}_{g',n'}(L')$ , where the exact type and boundaries of the ribbon graph complex in the image is one of the possibilities discussed before. The torus quotient is a local operation and any edge  $j$  not incident to  $i$  has  $q_*T_j = T_j$ , so it remains to find lifts of edges labeled  $k_1$  and  $k_2$  in Figure 9.

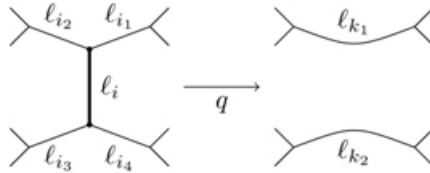


**Figure 9** Edge notation used to calculate the quotient symplectic form

It is clear that

$$q_*(T_{i_1} + T_{i_2}) = T_{k_1},$$

$$q_*(T_{i_3} + T_{i_4}) = T_{k_2}$$

and that

$$\begin{aligned} \Omega(T_{i_1} + T_{i_2}, \cdot) &= -2(d\ell_{i_1} + d\ell_{i_2}) \\ &= -2d\ell_{k_1}, \end{aligned}$$

$$\begin{aligned} \Omega(T_{i_3} + T_{i_4}, \cdot) &= -2(d\ell_{i_3} + d\ell_{i_4}) \\ &= -2d\ell_{k_2}. \end{aligned}$$

This completes the proof of the lemma. □

### 4. Recursion Formula

As constructed in the previous section, we have a partition of unity subordinate to the open cover

$$\{\mathcal{U}(\Gamma, i) \mid \Gamma \in \text{RG}_{g,n}^3(L), b(i) = 1\}.$$

Hence we wish to calculate the partition-scaled volume of each  $\mathcal{U}(\Gamma, i)$ . Rather than calculate each individually, we will group the covers together according to the type and boundary labelings of the edge-deleted graph  $\Gamma_{\hat{i}}$ . In particular, four different types arise as follows.

(1) Edge  $i$  bounds perimeters 1 and  $j$  for some  $j \neq 1$ . In this case, removing edge  $i$  is the same as removing a  $\theta$ -graph with boundary lengths  $(L_1, L_j, x)$  and leaving  $\Gamma_{\hat{i}} \in \text{RG}_{g,n-1}(x, L_{\underline{n} \setminus \{1,j\}})$ , where  $|L_1 - L_j| < x < L_1 + L_j$ . The length of the edge being removed (i.e., the value of the partition of  $L_1$ ) is calculated as

$$\ell_i = \frac{1}{2}(L_1 + L_j - x).$$

(2) Edge  $i$  is part of a lollipop, with boundaries 1 and  $j$  on either side (again,  $1 \neq j$ ). We have  $\Gamma_{\hat{i}} \in \text{RG}_{g,n-1}(x, L_{\underline{n} \setminus \{1,j\}})$ , where  $0 \leq x \leq |L_1 - L_j|$ . The total length of the lollipop (i.e., the sum of all edges that contribute to this term) is

$$\begin{cases} L_1 & \text{if } L_1 < L_j, \\ L_1 - x & \text{if } L_1 > L_j. \end{cases}$$

(3) Edge  $i$  has boundary 1 on both sides, neither vertex has a loop, and removing edge  $i$  does not disconnect the graph. Then  $\Gamma_{\hat{i}} \in \text{RG}_{g-1,n+1}(x, y, L_{\underline{n} \setminus \{1\}})$ , where  $0 < x + y < L_1$ . The length of edge  $i$  is calculated to be

$$\ell_i = \frac{1}{2}(L_1 - x - y).$$

(4) Edge  $i$  has boundary 1 on both sides, neither vertex is incident to a loop, but removing edge  $i$  disconnects the graph. Then  $\Gamma_{\hat{i}} \in \text{RG}_{g_1, n_1}(x, L_{\mathcal{I}}) \times \text{RG}_{g_2, n_2}(y, L_{\mathcal{J}})$ , where  $g_1 + g_2 = g$ ,  $\mathcal{I} \sqcup \mathcal{J} = \underline{n} \setminus \{1\}$ ,  $n_1 = |\mathcal{I}| + 1$ , and  $n_2 = |\mathcal{J}| + 1$ . The newly created boundaries satisfy  $0 < x + y < L_1$ , and the length of the removed edge is

$$\ell_i = \frac{1}{2}(L_1 - x - y).$$

We note for future reference that if  $g_1 = g_2$  and  $|\mathcal{I}| = 0 = |\mathcal{J}|$  then there is a symmetry of order 2 obtained by exchanging  $x$  and  $y$ .

We reiterate that there are multiple groupings coming from each of these four types. For example, pairs  $(\Gamma, i)$  satisfying type (1) with  $j = 2$  are in a different group than pairs satisfying type (1) with  $j = 3$ . Only type (3) describes a single group.

What makes the integration scheme work is that the symplectic quotients  $\mathcal{U}(\Gamma, i) // \mathbb{T}$  of a fixed type form a disjoint cover of the appropriate ribbon graph complex. In other words, the combined reduced volumes of a given type coincide with the volume of the ribbon graph complex of the specified type. This is most easily seen by working backwards. For instance, starting with a graph  $\Gamma \in \text{RG}_{g, n-1}(x, L_{\underline{n} \setminus \{1, j\}})$  and a point on the boundary of length  $x$ , there is a unique way to recover a graph in  $\text{RG}_{g, n}(L_{\underline{n}})$ : if  $x < |L_1 - L_j|$  then one must attach a lollipop to the marked point, and if  $x > |L_1 - L_j|$  then one must attach a theta graph to the marked point (one of the two vertices of the theta graph must be distinguished in order to perform this operation unambiguously). The other cases are similar.

To calculate the volume of  $\text{RG}_{g, n}(L_{\underline{n}})$ , we use the partition of unity to write the volume as a sum over torus covers  $\mathcal{U}(\Gamma, i)$ . We group the covers by type and use the symplectic volume equation (2.3) to calculate the contribution from each grouping. The result is that

$$\begin{aligned} &L_1 \text{Vol}_{g, n}(L_1, \dots, L_n) \\ &= \sum_{j=2}^n \int_{|L_1 - L_j|}^{L_1 + L_j} dx \frac{x}{2}(L_1 + L_j - x) \text{Vol}_{g, n-1}(L_{\underline{n} \setminus \{1, j\}}, x) \\ &\quad + \sum_{j=2}^n \int_0^{|L_1 - L_j|} dx x f(x, L_1, L_j) \text{Vol}_{g, n-1}(L_{\underline{n} \setminus \{1, j\}}, x) \\ &\quad + \iint_{0 \leq x + y \leq L_1} dx dy \frac{xy}{2}(L_1 - x - y) \text{Vol}_{g-1, n+1}(L_{\underline{n} \setminus 1}, x, y) \\ &\quad + \sum_{\substack{g_1 + g_2 = g \\ \mathcal{I} \sqcup \mathcal{J} = \underline{n} \setminus 1}} \iint_{0 \leq x + y \leq L_1} dx dy \frac{xy}{2}(L_1 - x - y) \\ &\quad \times \text{Vol}_{g_1, n_1}(L_{\mathcal{I}}, x) \text{Vol}_{g_2, n_2}(L_{\mathcal{J}}, y), \end{aligned} \tag{4.1}$$

where

$$f(x, y, z) = \begin{cases} y - x & \text{if } y > z, \\ y & \text{if } y < z. \end{cases}$$

In this formulation, each integral summand comes from one of the four groupings enumerated previously. The integrand consists of the product of periods of the torus action ( $x$  or  $xy$ ) multiplied by the appropriate weighting from the partition of unity (length of the edge being removed) times the volume of the symplectic quotient.

The term coming from case (3) has double the edge weighting because the edge appears twice when traversing the boundary. This factor of 2 is compensated by the factor of  $\frac{1}{2}$  that arises because, when removing the edge from a graph, there is no way to distinguish the two newly created boundaries. Thus,  $RG_{g-1, n+1}(x, y, L_{\underline{n} \setminus 1})$  is counted twice because the  $x$ -length boundary is distinguished from the  $y$ -length boundary.

The double-edge contribution in case (4) is compensated for because the sum over  $g_1 + g_2 = g$  and  $\mathcal{I} \sqcup \mathcal{J} = \underline{n} \setminus 1$  gives a double count over the groupings. The one exception is when  $g_1 = g_2$  and  $n = 1$ . This case only appears once (if at all) in the sum, but the factor of  $\frac{1}{2}$  is accounted for by the order-2 symmetry of the underlying graph.

Equation (4.1) is a *topological recursion* formula for the volumes. In particular, the types of the ribbon graphs appearing on the right-hand side (RHS) are simpler than the type on the left-hand side (LHS; recall from Section 3 that the complexity of a graph of type  $(g, n)$  can be measured by  $2g - 2 + n$ ). Implicit in this computation is that  $(g, n) \neq (0, 3), (1, 1)$ . These can be considered the base cases for the recursion, since all other volume computations can be reduced to knowing  $\text{Vol}_{0,3}(L_3)$  and  $\text{Vol}_{1,1}(L)$ . Fortunately, these complexes are simple enough that their volumes can be calculated by hand, which we now proceed to do.

**VOLUME OF  $RG_{0,3}(L_1, L_2, L_3)$ .** The ribbon graph complex of type  $(0, 3)$  has dimension  $6g - 6 + 2n = 0$ , so we are integrating  $\Omega^0 = 1$  over a 0-dimensional space. In other words,  $\text{Vol}_{0,3}(L_3)$  is a discrete count of metric ribbon graphs of specified perimeter lengths. The set of all ribbon graphs of type  $(0, 3)$  can be found in Figure 4. Note that the automorphism groups are all trivial. Furthermore, once the perimeters are fixed, there is a unique metric ribbon graph that realizes those perimeters.

In particular, if  $L_i + L_j > L_k$  for all distinct  $i, j, k$  then only the theta graph is possible. The set of perimeter equations

$$\begin{aligned} \ell_1 + \ell_2 &= L_1, \\ \ell_2 + \ell_3 &= L_2, \\ \ell_1 + \ell_3 &= L_3 \end{aligned}$$

has a unique solution with all  $\ell_i > 0$ . If for some  $i, j, k$  we have  $L_i + L_j = L_k$ , then the only possible graph is the figure eight with the two boundary loops labeled by  $i$  and  $j$ . Finally, if  $L_i + L_j < L_k$  for some  $i, j, k$  then the graph is a dumbbell with the two boundary loops labeled by  $i$  and  $j$ . We conclude that

$$\text{Vol}_{0,3}(L_1, L_2, L_3) = 1.$$

Observe that this is the only 0-dimensional ribbon graph complex, so it is the only case where a non-trivalent graph contributes to the volume.

**VOLUME OF  $\text{RG}_{1,1}(L)$ .** For graphs of type (1, 1), the dimension of the ribbon graph complex is  $6g - 6 + 2n = 2$ . Hence we integrate  $\Omega$  over  $\text{RG}_{1,1}(L)$ . As illustrated in Figure 3, there is a single graph with the correct number of edges and whose automorphism group is  $\mathbb{Z}_6$ . If the edges are labeled such that, when traversing the boundary, we encounter (in order)  $\ell_1, \ell_2, \ell_3, \ell_1, \ell_2, \ell_3$ , then

$$\Omega = d\ell_1 \wedge (d\ell_2 + d\ell_3) + d\ell_2 \wedge d\ell_3.$$

If we fix  $2(\ell_1 + \ell_2 + \ell_3) = L$ , then  $d\ell_3 = -d\ell_1 - d\ell_2$  and so

$$\Omega|_{\text{RG}_{1,1}(L)} = d\ell_1 \wedge d\ell_2;$$

thus we have

$$\iint_{\ell_1 + \ell_2 \leq L/2} \Omega = \frac{1}{8}L^2.$$

After dividing by the order of the automorphism group, we conclude that

$$\text{Vol}_{1,1}(L) = \frac{1}{48}L^2.$$

### 5. Virasoro Constraints

The DVV formula [6], or Virasoro constraints, for  $\psi$ -class intersections is

$$\begin{aligned} \langle \tau_{d_1} \cdots \tau_{d_n} \rangle_g &= \sum_{j=2}^n \frac{(2d_1 + 2d_j - 1)!!}{(2d_1 + 1)!! (2d_j - 1)!!} \langle \tau_{d_1+d_j-1} \tau_{d_n \setminus \{1, j\}} \rangle_g \\ &+ \frac{1}{2} \sum_{a+b=d_1-2} \frac{(2a + 1)!! (2b + 1)!!}{(2d_1 + 1)!!} \\ &\times \left[ \langle \tau_a \tau_b \tau_{d_n \setminus 1} \rangle_{g-1} + \sum_{\substack{\text{stable} \\ g_1+g_2=g \\ \mathcal{I} \sqcup \mathcal{J} = n \setminus 1}} \langle \tau_a \tau_{d_{\mathcal{I}}} \rangle_{g_1} \langle \tau_b \tau_{d_{\mathcal{J}}} \rangle_{g_2} \right], \end{aligned} \tag{5.1}$$

where we use the notation

$$\langle \tau_{d_1} \cdots \tau_{d_n} \rangle_g = \int_{\overline{\mathcal{M}}_{g,n}} \psi_1^{d_1} \cdots \psi_n^{d_n}$$

and where

$$(2k + 1)!! = (2k + 1)(2k - 1) \cdots 1 = \frac{(2k + 1)!}{2^k k!}.$$

The stable sum in the last term means we restrict to terms for which  $(g_i, n_i)$  satisfy  $2g_i - 2 + n_i > 0$ , where  $n_1 = |\mathcal{I}| + 1$  and  $n_2 = |\mathcal{J}| + 1$ .

The topological recursion formula (4.1) is equivalent to the DVV formula (5.1) when one looks at terms of fixed degree in the  $L_i$ . Toward that end, if  $P(L_{\underline{n}})$  is a polynomial in  $L_1^2, \dots, L_n^2$  then we denote by

$$[d_1 \cdots d_n]P(L_n)$$

the coefficient in  $P$  of the monomial  $L_1^{2d_1} \cdots L_n^{2d_n}$ . As seen in (2.1), we have

$$\begin{aligned} [d_1 \cdots d_n] \text{Vol}_{g,n}(L_n) &= \frac{1}{\prod 2^{d_i} d_i!} \int_{\overline{\mathcal{M}}_{g,n}} \psi_1^{d_1} \cdots \psi_n^{d_n} \\ &= \frac{1}{\prod 2^{d_i} d_i!} \langle \tau_{d_1} \cdots \tau_{d_n} \rangle_g, \end{aligned}$$

where the coefficient is nonzero if and only if  $d_1 + \cdots + d_n = d = 3g - 3 + n$ .

Note, however, that the topological recursion formula (4.1) has  $L_1 \text{Vol}_{g,n}$  on the left-hand side. In fact, it turns out to simplify the calculations if we consider the differentiated topological recursion equation—namely, differentiate both sides by  $L_1$ . Then the LHS gives

$$[d_1 \cdots d_n] \frac{\partial}{\partial L_1} L_1 \text{Vol}_{g,n}(L_n) = \frac{2d_1 + 1}{\prod 2^{d_i} d_i!} \langle \tau_{d_1} \cdots \tau_{d_n} \rangle_g. \tag{5.2}$$

The differentiated topological recursion formula becomes somewhat simpler:

$$\begin{aligned} &\frac{\partial}{\partial L_1} L_1 \text{Vol}_{g,n}(L_n) \\ &= \sum_{j=2}^n \int_0^{L_1+L_j} \frac{x}{2} \text{Vol}_{g,n-1}(x, L_n \setminus \{1, j\}) dx \\ &\quad + \sum_{j=2}^n \int_0^{|L_1-L_j|} \frac{x}{2} \text{Vol}_{g,n-1}(x, L_n \setminus \{1, j\}) dx \\ &\quad + \iint_{0 \leq x+y \leq L_1} \frac{xy}{2} \text{Vol}_{g-1,n+1}(x, y, L_n \setminus \{1\}) dx dy \\ &\quad + \sum_{\substack{g_1+g_2=g \\ \mathcal{I} \sqcup \mathcal{J} = \underline{n} \setminus \{1\}}} \iint_{0 \leq x+y \leq L_1} \frac{xy}{2} \text{Vol}_{g_1,n_1}(x, L_{\mathcal{I}}) \text{Vol}_{g_2,n_2}(y, L_{\mathcal{J}}) dx dy. \end{aligned} \tag{5.3}$$

In order to calculate the matching monomial coefficient on the RHS of this recursion formula, we must explicitly evaluate the integrals.

For a fixed integer  $k \geq 0$ , we have

$$\begin{aligned} &\int_0^{L_1+L_j} \frac{x}{2} x^{2k} dx + \int_0^{|L_1-L_j|} \frac{x}{2} x^{2k} dx \\ &= \frac{1}{2(2k+2)} (L_1 + L_j)^{2k+2} + \frac{1}{2(2k+2)} (L_1 - L_j)^{2k+2} \\ &= \frac{1}{2(2k+2)} \sum_{r=0}^{2k+2} \binom{2k+2}{r} [L_1^r L_j^{2k+2-r} + (-1)^r L_1^r L_j^{2k+2-r}] \\ &= \sum_{s=0}^{k+1} \frac{(2k+1)!}{(2s)! (2k+2-2s)!} L_1^{2s} L_j^{2(k+1-s)}. \end{aligned} \tag{5.4}$$

By comparing degrees, we see that the coefficient of the  $[d_1 \cdots d_n]$  term coming from the integration is equal to

$$\begin{aligned} & \frac{(2(d_1 + d_j) - 1)!}{(2d_1)! (2d_j)!} \left[ d_1 + d_j - 1 \prod_{i \neq 1, j} d_i \right] \text{Vol}_{g, n-1}(x, L_{\underline{n} \setminus \{1, j\}}) \\ &= \frac{(2(d_1 + d_j) - 1)!}{(2d_1)! (2d_j)!} \frac{\langle \tau_{d_1+d_j-1} \tau_{\underline{n} \setminus \{1, j\}} \rangle_g}{2^{d_1+d_j-1} 2^{d_n \setminus \{1, j\}} (d_1 + d_j - 1)! d_{\underline{n} \setminus \{1, j\}}!}. \end{aligned}$$

We also calculate the double integrals by fixing integers  $a, b \geq 0$ :

$$\iint_{0 \leq x+y \leq L_1} \frac{xy}{2} x^{2a} y^{2b} dx dy = \frac{1}{2} \frac{(2a + 1)! (2b + 1)!}{(2(a + b + 2))!} L_1^{2(a+b+2)}.$$

Hence terms containing  $L_1^{2d_1}$  must have  $a + b = d_1 - 2$ .

Assembling the individual contributions yields

$$\begin{aligned} & \frac{2d_1 + 1}{\prod 2^{d_i} d_i!} \langle \tau_{d_1} \cdots \tau_{d_n} \rangle_g \\ &= \sum_{j=2}^n \frac{(2(d_1 + d_j) - 1)!}{(2d_1)! (2d_j)!} \frac{\langle \tau_{d_1+d_j-1} \prod_{i \neq 1, j} \tau_{d_i} \rangle_g}{2^{d_1+d_j-1} (d_1 + d_j - 1)! \prod_{i \neq 1, j} 2^{d_i} d_i!} \\ &+ \frac{1}{2} \sum_{a+b=d_1-2} \frac{(2a + 1)! (2b + 1)!}{(2d_1)!} \frac{1}{2^a a! 2^b b!} \frac{1}{\prod_{i \neq 1} 2^{d_i} d_i!} \\ &\times \left[ \left\langle \tau_a \tau_b \prod_{i \neq 1} \tau_{d_i} \right\rangle_{g-1} + \sum_{\substack{g_1+g_2=g \\ \mathcal{I} \sqcup \mathcal{J} = \underline{n} \setminus \{1\}}} \left\langle \tau_a \prod_{i \in \mathcal{I}} \tau_{d_i} \right\rangle_{g_1} \left\langle \tau_b \prod_{i \in \mathcal{J}} \tau_{d_i} \right\rangle_{g_2} \right]. \end{aligned}$$

After matching terms are canceled, using the relation

$$(2k - 1)!! = \frac{(2k)!}{2^k k!}$$

gives the DVV equation (5.1).

We remark that [26; 31; 34] all obtained the same results, in some cases using similar ideas. However, in those works a scaling limit argument is required to access the  $\psi$ -class terms. Deriving the DVV is much simpler in this paper because no rescaling is necessary.

### 6. Eynard–Orantin Recursion

In this section we prove that the topological recursion formula (4.1) is equivalent to the Eynard–Orantin recursion for the spectral curve  $x = \frac{1}{2}y^2$ . The main idea is to take the Laplace transform of the recursion formula.

To that end, we define

$$W_{g,n}(z_1, \dots, z_n) = \int \cdots \int e^{-z_n \cdot L_n} L_1 \cdots L_n \text{Vol}_{g,n}(L_1, \dots, L_n) dL_1 \cdots dL_n,$$

where  $z_n \cdot L_n = z_1 L_1 + \dots + z_n L_n$  and the integration is performed over  $[0, \infty)^n$ . If we take the Laplace transform of  $L_2 \cdots L_n$  times the recursion formula then the LHS becomes  $W_{g,n}(z_1, \dots, z_n)$ . We evaluate the integrals on the RHS by swapping the order of integration, as explained next.

In general, if  $V(x, y)$  denotes a polynomial in  $x^2$  and  $y^2$  and if

$$W(z_1, z_2) = \int_0^\infty \int_0^\infty e^{-xz_1 - yz_2} xy V(x, y) dx dy,$$

then

$$\begin{aligned} & \int_0^\infty dL_1 e^{-z_1 L_1} \iint_{0 \leq x+y \leq L_1} dx dy xy (L_1 - x - y) V(x, y) \\ &= \int_0^\infty dx \int_0^\infty dy \int_{x+y}^\infty dL_1 xy \left( -\frac{\partial}{\partial z_1} - (x+y) \right) e^{-z_1 L_1} V(x, y) \\ &= \frac{1}{z_1^2} \int_0^\infty dx \int_0^\infty dy xy V(x, y) e^{-z_1 x - z_1 y} \\ &= \frac{1}{z_1^2} W(z_1, z_1). \end{aligned} \tag{6.1}$$

For the term involving boundary  $j$ , we define

$$F(x, L_1, L_j) = \begin{cases} L_1 & \text{if } L_1 < L_j, x < L_j - L_1, \\ L_1 - x & \text{if } L_j < L_1, x < L_1 - L_j, \\ \frac{1}{2}(L_1 + L_j - x) & \text{if } |L_1 - L_j| < x < L_1 + L_j \end{cases}$$

and then calculate

$$\begin{aligned} & \int_0^\infty dL_j L_j e^{-z_j L_j} \int_0^\infty dL_1 e^{-z_1 L_1} \int_0^{L_1+L_j} dx x F(x, L_1, L_j) V(x) \\ &= -\frac{\partial}{\partial z_j} \left[ \frac{1}{z_1^2 z_j (z_1^2 - z_j^2)} (z_1^2 W(z_j) - z_j^2 W(z_1)) \right]; \end{aligned} \tag{6.2}$$

here again we have adopted the convention that  $W(z)$  is the Laplace transform of  $xV(x)$  under the assumption that  $V(x)$  is a polynomial in  $x^2$ . This equation can be verified by Mathematica, and it is easy to calculate by hand if one swaps the order of integration and introduces the change of variables

$$\begin{aligned} u &= L_1 + L_j - x, \\ v &= L_j - L_1. \end{aligned}$$

Coming back to the topological recursion formula (4.1), we use (6.2) to calculate the Laplace transform of the first line of the formula and use (6.1) for the remainder of the terms. The result is the following recursion formula for  $W_{g,n}$ .

LEMMA 6.1. *We have*

$$\begin{aligned}
 W_{g,n}(z_n) &= \sum_{j=2}^n -\frac{\partial}{\partial z_j} \left[ \frac{z_j}{(z_1 z_j)^2 (z_1^2 - z_j^2)} (z_1^2 W_{g,n-1}(z_{n \setminus 1}) - z_j^2 W_{g,n-1}(z_{n \setminus j})) \right] \\
 &\quad + \frac{1}{2z_1^2} W_{g-1,n+1}(z_1, z_n) \\
 &\quad + \frac{1}{2z_1^2} \sum_{\substack{g_1+g_2=g \\ \mathcal{I} \sqcup \mathcal{J} = n \setminus 1}} W_{g_1,n_1}(z_1, z_{\mathcal{I}}) W_{g_2,n_2}(z_1, z_{\mathcal{J}}), \tag{6.3}
 \end{aligned}$$

where  $n_1 = |\mathcal{I}| + 1$ ,  $n_2 = |\mathcal{J}| + 1$ , and the summation in the last line is taken over all pairs  $(g_1, \mathcal{I})$  and  $(g_2, \mathcal{J})$  subject to the stability condition  $2g_i - 2 + n_i > 0$ .

The goal is to equate this recursion formula to Eynard–Orantin recursion for the Airy curve  $x = \frac{1}{2}y^2$ . To do so, we must explicitly evaluate the residues involved in (2.2). As a starting point, given a function  $W(\zeta_1, \zeta_2)$  that is assumed to be a polynomial in  $\zeta_1^{-2}$  and  $\zeta_2^{-2}$ , we have

$$\begin{aligned}
 \operatorname{Res}_{\zeta \rightarrow 0} E(\zeta, z_1) W(\zeta, -\zeta) d\zeta \otimes d(-\zeta) &= \operatorname{Res}_{\zeta \rightarrow 0} \frac{-1}{2\zeta} \frac{1}{\zeta^2 - z_1^2} W(\zeta, \zeta) d\zeta \otimes dz_1 \\
 &= \frac{1}{2z_1^2} W(z_1, z_1) dz_1.
 \end{aligned}$$

Recall that the Eynard kernel  $E(\zeta, z_1)$  is

$$E(\zeta, z_1) = \frac{1}{2\zeta(\zeta^2 - z_1^2)} \frac{1}{d\zeta} \otimes dz_1.$$

The unstable terms in the Eynard–Orantin recursion have a more complicated residue calculation because of the diagonal pole in  $W_{0,2}$ . We have

$$\begin{aligned}
 \operatorname{Res}_{\zeta \rightarrow 0} E(\zeta, z_1) (W_{0,2}(\zeta, z_j) W(-\zeta) + W_{0,2}(-\zeta, z_j) W(\zeta)) d\zeta \otimes d(-\zeta) \\
 &= \operatorname{Res}_{\zeta \rightarrow 0} \frac{1}{2\zeta} \frac{-1}{\zeta^2 - z_1^2} \left[ \frac{1}{(\zeta - z_j)^2} + \frac{1}{(\zeta + z_j)^2} \right] W(\zeta) d\zeta \otimes dz_1 \\
 &= \operatorname{Res}_{\zeta \rightarrow 0} \frac{1}{\zeta(z_1^2 - \zeta^2)} \left[ -\frac{\partial}{\partial z_j} \frac{z_j}{z_j^2 - \zeta^2} \right] W(\zeta) d\zeta \otimes dz_1,
 \end{aligned}$$

where we assume that  $W(\zeta)$  is a polynomial in  $\zeta^{-2}$ . To finish the calculation, we use our next lemma.

LEMMA 6.2. *For any integer  $k \geq 0$ ,*

$$\operatorname{Res}_{\zeta \rightarrow 0} \frac{1}{\zeta} \frac{1}{z_1^2 - \zeta^2} \frac{1}{z_j^2 - \zeta^2} \zeta^{-2k} d\zeta = \frac{1}{z_1^2 z_j^2 (z_1^2 - z_j^2)} (z_1^2 z_j^{-2k} - z_j^2 z_1^{-2k}).$$

*Proof.* We expand the LHS while assuming that  $\zeta$  is closer to 0 than are both  $z_1$  and  $z_j$ :

$$\begin{aligned}
& \operatorname{Res}_{\zeta \rightarrow 0} \frac{1}{z_1^2 - \zeta^2} \frac{1}{z_j^2 - \zeta^2} \zeta^{-2k-1} d\zeta \\
&= \operatorname{Res}_{\zeta \rightarrow 0} \frac{1}{z_1^2 z_j^2} \left(1 + \frac{\zeta^2}{z_1^2} + \dots\right) \left(1 + \frac{\zeta^2}{z_j^2} + \dots\right) \zeta^{-2k-1} d\zeta \\
&= \frac{1}{z_1^2 z_j^2} \sum_{r+s=k} z_1^{-2r} z_j^{-2s} \\
&= \frac{z_1^2 - z_j^2}{z_1^2 z_j^2 (z_1^2 - z_j^2)} \sum_{r=0}^k z_1^{-2r} z_j^{-2(k-r)} \\
&= \frac{1}{z_1^2 z_j^2 (z_1^2 - z_j^2)} (z_1^2 z_j^{-2k} - z_1^{-2k} z_j^2). \quad \square
\end{aligned}$$

Putting everything together gives us the following statement.

**THEOREM 6.3.** *The topological recursion formula (4.1) for the symplectic volume of the ribbon graph complex is equivalent to the Eynard–Orantin recursion for the spectral curve  $x = \frac{1}{2}y^2$ .*

## References

- [1] G. Borot, B. Eynard, M. Mulase, and B. Safnuk, *A matrix model for simple Hurwitz numbers, and topological recursion*, J. Geom. Phys. 61 (2011), 522–540.
- [2] V. Bouchard, A. Klemm, M. Mariño, and S. Pasquetti, *Remodeling the B-model*, Comm. Math. Phys. 287 (2009), 117–178.
- [3] V. Bouchard and M. Mariño, *Hurwitz numbers, matrix models and enumerative geometry*, From Hodge theory to integrability and TQFT tt\*-geometry, Proc. Sympos. Pure Math., 78, pp. 263–283, Amer. Math. Soc., Providence, RI, 2008.
- [4] B. H. Bowditch and D. B. A. Epstein, *Natural triangulations associated to a surface*, Topology 27 (1988), 91–117.
- [5] K. M. Chapman, M. Mulase, and B. Safnuk, *The Kontsevich constants for the volume of the moduli of curves and topological recursion*, preprint, 2010, arXiv:1009.2055.
- [6] R. Dijkgraaf, E. Verlinde, and H. Verlinde, *Loop equations and Virasoro constraints in nonperturbative two-dimensional quantum gravity*, Nuclear Phys. B 348 (1991), 435–456.
- [7] J. J. Duistermaat and G. J. Heckman, *On the variation in the cohomology of the symplectic form of the reduced phase space*, Invent. Math. 69 (1982), 259–268.
- [8] B. Eynard, *Recursion between Mumford volumes of moduli spaces*, preprint, 2007, arXiv:0706.4403.
- [9] ———, *All order asymptotic expansion of large partitions*, J. Stat. Mech. Theory Exp. 9 (2008), P07023.
- [10] ———, *A matrix model for plane partitions*, J. Stat. Mech. Theory Exp. 10 (2009), P10011.
- [11] B. Eynard, A. K. Kashani-Poor, and O. Marchal, *A matrix model for the topological string I: Deriving the matrix model*, preprint, 2010, arXiv:1003.1737.
- [12] B. Eynard, M. Mulase, and B. Safnuk, *The Laplace transform of the cut-and-join equation and the Bouchard–Marino conjecture on Hurwitz numbers*, Publ. Res. Inst. Math. Sci. 47 (2011), 629–670.

- [13] B. Eynard and N. Orantin, *Invariants of algebraic curves and topological expansion*, Commun. Number Theory Phys. 1 (2007), 347–452.
- [14] ———, *Weil–Petersson volume of moduli spaces, Mirzakhani’s recursion and matrix models*, preprint, 2007, arXiv:0705.3600.
- [15] ———, *Topological recursion in enumerative geometry and random matrices*, J. Phys. A 42 (2009), 293001.
- [16] ———, *Geometrical interpretation of the topological recursion, and integrable string theories*, preprint, 2009, arXiv:0911.5096.
- [17] V. Guillemin and S. Sternberg, *Convexity properties of the moment mapping*, Invent. Math. 67 (1982), 491–513.
- [18] J. L. Harer, *The cohomology of the moduli space of curves*, Theory of moduli (Montecatini Terme, 1985), Lecture Notes in Math., 1337, pp. 138–221, Springer-Verlag, Berlin, 1988.
- [19] M. E. Kazarian and S. K. Lando, *An algebro-geometric proof of Witten’s conjecture*, J. Amer. Math. Soc. 20 (2007), 1079–1089.
- [20] Y.-S. Kim and K. Liu, *A simple proof of Witten conjecture through localization*, preprint, 2005, arXiv:math/0508384.
- [21] M. Kontsevich, *Intersection theory on the moduli space of curves and the matrix Airy function*, Comm. Math. Phys. 147 (1992), 1–23.
- [22] K. Liu and H. Xu, *New properties of the intersection numbers on moduli spaces of curves*, Math. Res. Lett. 14 (2007), 1041–1054.
- [23] ———, *New results of intersection numbers on moduli spaces of curves*, Proc. Natl. Acad. Sci. USA 104 (2007), 13896–13900.
- [24] ———, *Recursion formulae of higher Weil–Petersson volumes*, Int. Math. Res. Not. 5 (2009), 835–859.
- [25] M. Mirzakhani, *Simple geodesics and Weil–Petersson volumes of moduli spaces of bordered Riemann surfaces*, Invent. Math. 167 (2007), 179–222.
- [26] ———, *Weil–Petersson volumes and intersection theory on the moduli space of curves*, J. Amer. Math. Soc. 20 (2007), 1–23.
- [27] M. Mulase and M. Penkava, *Ribbon graphs, quadratic differentials on Riemann surfaces, and algebraic curves defined over  $\mathbb{Q}$* , Asian J. Math. 2 (1998), 875–919.
- [28] ———, *Topological recursion for the Poincaré polynomial of the combinatorial moduli space of curves*, preprint, 2010, arXiv:1009.2135.
- [29] M. Mulase and B. Safnuk, *Mirzakhani’s recursion relations, Virasoro constraints and the KdV hierarchy*, Indian J. Math. 50 (2008), 189–218.
- [30] ———, *Combinatorial structures in topological recursion*, in preparation.
- [31] M. Mulase and N. Zhang, *Polynomial recursion formula for linear Hodge integrals*, Commun. Number Theory Phys. 4 (2010), 267–293.
- [32] P. Norbury, *Counting lattice points in the moduli space of curves*, preprint, 2008, arXiv:0801.4590.
- [33] ———, *String and dilaton equations for counting lattice points in the moduli space of curves*, Math. Res. Lett. 17 (2010), 467–481.
- [34] A. Okounkov and R. Pandharipande, *Gromov–Witten theory, Hurwitz numbers, and matrix models*, Algebraic geometry (Seattle, 2005), Proc. Sympos. Pure Math., 80, pp. 325–414, Amer. Math. Soc., Providence, RI, 2009.
- [35] R. C. Penner, *The decorated Teichmüller space of punctured surfaces*, Comm. Math. Phys. 113 (1987), 299–339.
- [36] B. Safnuk, *Integration on moduli spaces of stable curves through localization*, Differential Geom. Appl. 27 (2009), 179–187.

- [37] ———, *Generalizations of topological recursion*, in preparation.
- [38] D. D. Sleator, R. E. Tarjan, and W. P. Thurston, *Rotation distance, triangulations, and hyperbolic geometry*, J. Amer. Math. Soc. 1 (1988), 647–681.
- [39] E. Witten, *Two-dimensional gravity and intersection theory on moduli space*, Surveys in differential geometry (Cambridge, MA, 1990), pp. 243–310, Lehigh Univ., Bethlehem, PA, 1991.

J. Bennett  
Department of Mathematics  
Bard College  
Annandale-on-Hudson, NY 12504  
juliacbennett@gmail.com

B. Safnuk  
Department of Mathematics  
Central Michigan University  
Mount Pleasant, MI 48859  
brad.safnuk@cmich.edu

D. Cochran  
Department of Mathematics  
Virginia Commonwealth University  
Richmond, VA 23220  
dcochran@math.utexas.edu

K. Woskoff  
Department of Mathematics  
Hartwick College  
Oneonta, NY 13820  
kwoskof@clemsun.edu